Bulletin of the Seismological Society of America, Vol. 83, No. 6, pp. 1939–1958, December 1993

VARIATION IN MICROSEISM POWER AND DIRECTION OF APPROACH IN NORTHEAST GREENLAND

BY P. E. HARBEN AND E. HJORTENBERG

ABSTRACT

Previous work on background noise at seismic stations in Greenland has shown minimum seismic noise in the winter months for frequencies around 1 Hz and maximum seismic noise in the winter months for periods around 6 sec. We have analyzed microseism data from three new digital seismic stations installed during the summer of 1991 in northeast Greenland at Nord, Daneborg, and Scoresbysund. We determined seasonal and station-to-station variations in spectral power density between August and December in the frequency band between 10 sec periods and 5-Hz frequencies. These variations are in agreement with previous studies at periods of 1 and 6 sec. During the summer months, all three stations recorded a minimum for the average spectral power density in the microseism band between 10- and 5-sec periods. From about 3-sec periods to at least 5-Hz frequencies, the average spectral power density is at a maximum during the summer at all three stations. Conversely, the winter months have a maximum in spectral power density between 10- and 5-sec periods and a minimum between about 3-sec periods and at least 5-Hz frequencies at all stations. Station-to-station average-spectral-power-density comparisons show that Nord and Daneborg are roughly comparable over most of the frequency band between 10-sec periods and at least 5-Hz frequencies. Scoresbysund has a systematically higher spectral power density between 8-sec periods and at least 5-Hz frequencies. Overall, Nord had the lowest background seismic noise, at some frequencies approaching the values of a low noise model.

We determined average direction of approaches in the 8- to 4-sec period band for each station during the months of August and November; these determinations agreed with previous studies. The predominant average direction of approaches were: southwest for Nord, south for Daneborg, and southeast for Scoresbysund. Although the microseism amplitude is larger and the direction-of-approach scatter is smaller during the winter months at all three stations, the direction-of-approach mean is apparently independent of season. A large number of storms develop around Iceland and typically track northeast, giving rise to large amplitude microseisms at Scoresbysund but relatively small amplitude microseisms at Daneborg and no microseism activity at Nord. This complete lack of microseism energy at Nord (and to a lesser degree Daneborg) from known frequent microseism sources in the Greenland Sea is shown for one 5-day period in August 1991. Other studies have shown that thick sediments in the Atlantic Ocean's continental margins are responsible for the absence of short-period surface waves from mid-ocean ridge earthquakes that have paths traversing such continental margins. Thick sediments act to attenuate, scatter, and disperse short-period surface waves. Indirect evidence indicates that the northeast Greenland shelf has thick and variable sediment layers. Because the paths of surface waves to Nord (and to a lesser extent Daneborg) originating from typical storms in the Greenland Sea have long path lengths traversing the northeast Greenland shelf, we conclude that this is the likely explanation for the lack of southeast directions from Nord (and to a lesser degree Daneborg) in the observed microseism direction of approaches.

INTRODUCTION

As early as the latter half of the nineteenth century, microseisms were thought to be associated with storms at sea. Although many theories sought to explain the connection between atmospheric disturbances at sea and microseism generation, perhaps the most obvious explanation was overlooked primarily because of two fundamental theoretical objections. First, linear first-order Stokes theory predicts that pressure fluctuations resulting from water waves will diminish exponentially with depth; therefore, waves raised by high winds from a large storm could not produce pressure fluctuations on the sea floor that results in microseism generation. Second, the relatively small wavelength of ocean waves would essentially cancel the pressure fluctuations over any area of the sea floor with a diameter much greater than one ocean wavelength at the surface.

In 1950, Longuet-Higgins published a paper that dispensed with these theoretical objections. He proposed a theory that described the physical mechanism underlying the coupling of ocean water waves to surface elastic wave energy. He argued that the coherent transfer of energy from water waves at sea to elastic waves is the consequence of a nonlinear, in-phase, unattenuated pressure fluctuation on the sea floor resulting from water wave interference. Thus, a microseism source is characterized by high amplitude surface water waves moving in opposite directions that give rise to relatively high amplitude standing surface water waves over a substantial region (much greater than a surface water wavelength). Hasselmann (1963) generalized the treatment of microseism generation by statistically analyzing the relations between the power spectra of the generating field and the microseism field. He found appreciable microseism generation only when the Fourier components of the random generation field have the same phase velocities as free modes of the elastic system.

The high Arctic in northeast Greenland provides a unique environment in which to measure and study the microseism activity with storms at sea. Standing water waves that generate microseisms detected at coastal seismic stations can be caused by cyclone movement at sea or by high amplitude waves reflecting off the coastline. Often the study of storm-related microseisms is complicated because both types of microseism sources are present during a typical storm period; this results in highly distributed sources. Microseisms recorded at stations in the high Arctic simplify the study of microseisms because the perennial coastal ice pack eliminates the possibility of local coastal wave reflection mechanisms as sources of microseism activity (although some wave reflection could occur at the ice pack margins) and because microseisms are not generated north of the permanent ice pack. Microseisms recorded at these stations are almost exclusively from distant sources at sea with approach directions limited to between about 90° and 270°. This part of Greenland also lacks vegetation, running water (during most of the year), and significant cultural activity; all of which contribute a very low seismic noise environment at higher frequencies ($\sim$ 1 Hz and above).

In this study, we have taken advantage of the fact that the direction of approach for northeast Greenland stations is less complex, because of the presence of permanent pack ice, than stations located to the south; thus, simplifying the study of station location and geological setting correlations. We study variations of seismic noise power in the 10-sec period to the 5-Hz frequency band and the microseism direction of approaches in the 8- to 4-sec

period band. In the 8- to 4-sec microseism band, we correlate the power and direction-of-approach variations with the physical location and the surrounding environment at the stations. The data analyzed here includes measurements from three digital seismic stations recently installed in northeast Greenland at stations Nord (NOR), Daneborg (DBG), and Scoresbysund (SCO). The locations of these and other seismic stations that will be discussed are shown in Figure 1.

Historical Microseism Studies in Greenland

Using seismic recordings from Kap Tobin (station KTG, located within 10 km of SCO) and Danmarkshavn (DAG) in northeast Greenland, Hjortenberg and Hjelme (1980) calculated a seasonal variation of seismic noise of 0.75 to 1.4 Hz for the year 1975. Their method consisted of determining the highest daily peak-to-peak trace amplitude of the noise in a 1-min period every 15 min. The results of Hjortenberg and Hjelme show that DAG had the lowest noise and relatively little seasonal variation, whereas station KTG had higher noise and significant seasonal variation. The maximum noise at both stations occurred between July and September. This seasonal variation can be attributed to local wave action, which is present in the summer but is suppressed in the winter by the sea ice pack. Station DAG, being much further north, has less sea ice melt in the summer months and a shorter period of open water in its vicinity than station KTG; consequently, the seasonal variation of 1-Hz noise was less pronounced. These changes of 1-Hz noise have also been observed in Antarctica (MacDowall, 1959) and in Canada (Basham and Whitham, 1966).

Lehmann (1952) studied a number of specific microseism storms that were measured at two Greenland seismic stations, SCO and Ivigtut (IVI), during the years 1949 to 1951. In this paper, she observes that, in a general way, the microseisms depend on the weather. She divides the seas into three regions: region 1. The Atlantic Ocean south of Greenland; region 2. The Atlantic Ocean south of Iceland and east of Greenland; and region 3. The Greenland and Norwegian Seas. Lehmann found no examples of cyclones occurring west of Greenland in the Davis Strait or Baffin Bay that gave rise to measurable microseisms at SCO or IVI. Cyclones passing through region 1 rarely moved inland because of the high terrain (over 2000 m); instead, they either moved around the coast to the east or split between the east and west coasts. Recordings of such cyclones at these two stations reveal: (1) relatively small-amplitude mixed-period microseisms caused by surf- and coast-reflected standing waves that result in shorter period microseisms and (2) microseisms generated at sea to the south and east of Greenland that result in longer period microseisms.

In region 2, the longest period microseisms (up to 8 sec) were observed at both SCO and IVI. Lehmann explains microseism period as related to and (all other parameters being equal) varying in accordance with the ocean depth in the region of microseism generation. The ocean is deep over a very large area of region 2; consequently, although a coastal effect is possible, the predominant microseism generation mechanism is in the open ocean. The IVI station always recorded higher amplitude microseisms than did the SCO station. IVI also recorded the maximum amplitude well after the time that the center of the cyclone made its closest approach to the station. Furthermore, when a cyclone's center was an equal distance from IVI and SCO, the microseism amplitudes recorded at IVI were much higher. Lehmann concludes that the cyclone's center is not the area of predominant microseism generation.

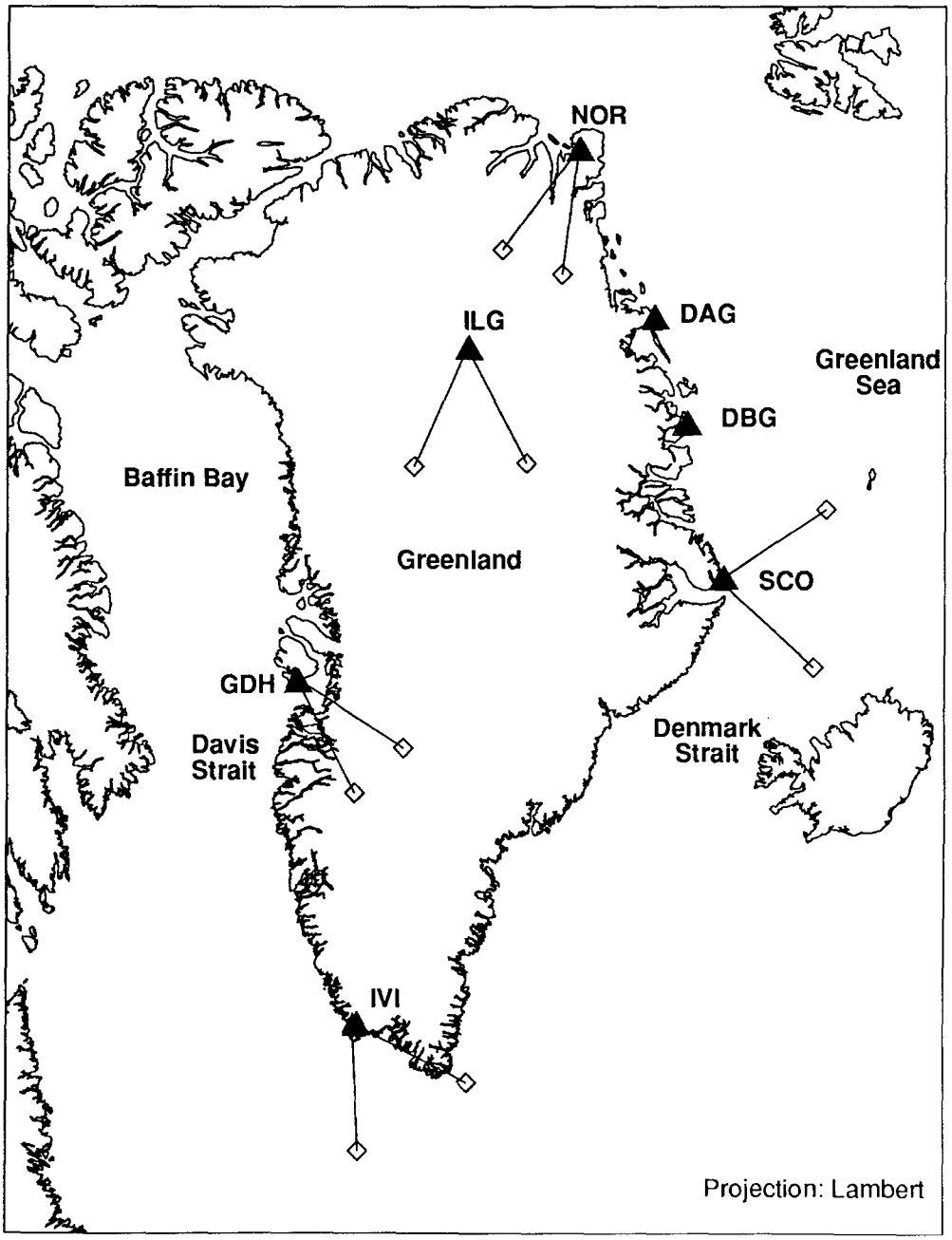

FIG. 1. The locations and identifiers of all Greenland seismic stations referenced in this study. Those stations with previous direction-of-approach results are shown with the minimum angle containing 50% of all direction of approaches calculated.

In region 3, Lehmann notes that, except for a few months in summer, there can be no microseism generation caused by coastal effects in northeast Greenland because of the extensive ice pack at sea. The author further states that polar air masses moving south tend to parallel the northeast Greenland coast. Cyclones in this region usually come from around Iceland and track east or northeast. Microseisms generated by such storms must be from waves at sea.

Microseism storms recorded at SCO do not reach a maximum when the cyclone's center is closest to the station, rather, the maximum is reached 6 h or more after the closest approach time. This is consistent with observations in region 2, and Lehmann concludes that the most active area of microseism generation from a cyclone at sea east of Greenland does not occur at the cyclone's center; instead, it occurs behind the cold front and between the cyclone's center and the Greenland coast.

Finally, Lehmann reports a general seasonal variation in the overall period and amplitude of microseisms in Greenland. During the summer months, dominant periods are typically 4- to 5 sec and of relatively low amplitude. The typical microseism sources are near the coast, and the weather is dominated by a stable high over Greenland. During the spring, fall, and winter months, the microseism amplitudes are high and the dominant periods are longer (5 to 7 sec). The weather consists mostly of extended storms over the seas surrounding Greenland, giving rise to microseisms generated in the deep ocean.

Seven microseism storms during the years 1949 and 1950 were analyzed by Båth (1953) using microseisms recorded in the 4- to 8-sec range at seismic stations in Greenland, Iceland, and Scandinavia. The Greenland station was at SCO. The author did not find any instances of a coastal effect in the generation of microseisms recorded at SCO (although a coastal effect on the Norwegian coastline was determined to be the dominant mechanism for the generation of microseisms recorded in Scandinavia). Consistent with Lehmann (1952), Båth concludes that the sea ice and the tendency for high winds to move parallel to the coastline of northeast Greenland preclude a coastal effect. The author also notes that in almost all cases, microseism amplitude maxima at SCO occurred well after the cyclone's center had passed its closest approach point to SCO. He also observes that maximum microseism amplitudes occurred when the polar winds behind the cyclone's center were well developed and blowing from the north over the open ocean east of SCO. Based on these observations, Båth concludes that polar winds in conjunction with a cyclone are somehow responsible for the generation of microseisms recorded at SCO and that the region of microseism generation is west of the cyclone's center.

Jensen (1957, 1958, 1961, and 1965) studied the Rayleigh-wave-component direction of approach of microseisms at four seismic stations in Greenland: NOR, SCO, IVI, and Godhavn (GDH). Direction of approaches were determined using the empty half-plane method. In this method, north–south and east–west recorded time derivatives were read at times when the vertical record component was at its maximum, and the phase relation was calculated. A number of such readings were averaged to minimize the errors possible from Love-wave components with assumed random phase relation to the Rayleigh-wave component of the microseism.

Jensen's results show that: For NOR, 50% of all direction of approaches determined over a 1-yr interval were between 215° and 244° from the station; For SCO, 50% were between 78° and 154°; For IVI, 50% were between 115° and 175°; For GDH, 50% were between 115° and 145°; and For the temporary seismic station (ILG) located on the central Greenland ice cap, 50% were between about 158° and 210° (Hjortenberg, 1970). These results are summarized in Figure 1. Jensen concludes that very few microseisms are recorded at Nord that originate in the southeast and that Nord is better characterized as an inland station than as a coastal station.

Recent Seasonal Spectra Comparisons

For this study, we analyzed seismic noise measurements from the new digital seismic stations (NOR, DBG, and SCO) to determine the seasonal and station-to-station variations in seismic noise power from the 10-sec period band to the 5-Hz frequency band. We compared our results with earlier studies based on more limited seismic bandwidths.

All spectral comparisons and monthly direction-of-approach comparisons were calculated from daily 5-min seismic noise samples taken at 0300 GMT at all three stations. We compared the averaged-acceleration power-density spectra at each station for the months August to December (only through November at DBG) to determine the average background-noise power and seasonal variability in the bands of interest. The spectra are a logarithmic average of the daily 5-min background noise records. We chose the 5-min time interval because it provided a sufficient time period for analysis in our chosen frequency bands. The recording time of 0300 GMT was chosen as a time when local cultural activity should be at a minimum. Three-component sets of Teledyne Geotech model GS-13 seismometers (Teledyne Geotech, Garland, TX) were used at all stations. These seismometers have a free period of 1 Hz. All data were corrected for instrument response and rolloff below 1 Hz. The corrected data from these seismometers can be used in low noise regions for periods of at least 12 sec and frequencies well above 5 Hz (Rodgers, 1991). The data were collected with Reftek-72 digital recorders.

Acceleration power-density spectra were calculated by converting the instrument-corrected velocity time waveform to acceleration. The correlation function was then calculated using a 50-sec window length and 12 windows. The power density spectra were calculated from the correlation function.

For periods from 10 sec or greater to about 6 sec, station NOR (Fig. 2a) shows a systematic increase in the average power density between August and November. Between about 5 to 3 sec, the trend reverses such that there is a systematic decrease in average power density between about 3 sec and at least 5 Hz. It seems that for frequencies between 1 Hz and at least 5 Hz, winter-condition background-noise levels are reached in October, with almost identical average levels in November.

Station DBG (Figure 2b) shows seasonal trends similar to NOR. Microseism noise at periods from at least 10 sec to about 5 sec has a much higher average power density during winter conditions compared to summer conditions. The trend reverses, as at NOR, for periods from about 2 sec to frequencies of at least 5 Hz.

The seasonal variation at SCO (Figure 2c) shows the same seasonal trends in about the same frequency bands as NOR and DBG. For periods between 6 sec and at least 10 sec, SCO shows a systematic increase in the average power density between August and December. This trend reverses such that, between about 2 sec and at least 5 Hz, there is a significant decrease in average power density between summer and winter conditions. The winter-condition noise levels do not appear to begin until the month of November. By December, the winter-condition noise levels are fully established.

The mean-background seismic-noise variation between summer and winter conditions observed in this study is in agreement with the result of Hjortenberg and Hjelme (1980) in the 0.75 to 1.4 Hz band at SCO and shows a similar trend at NOR. Our results extend the frequency band of this trend from about 2 to 3

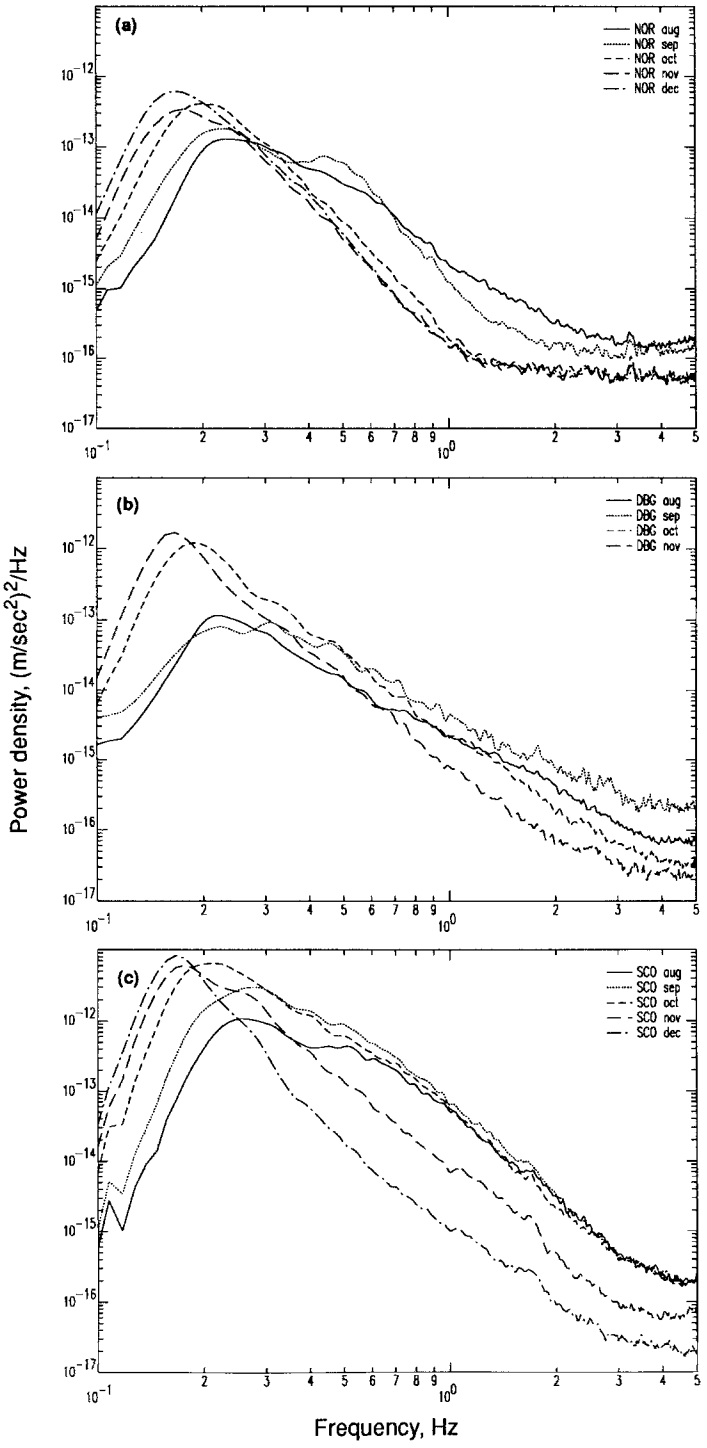

FIG. 2. The logarithmic averaged-acceleration power-density spectra for the months August to December, 1991 (only August to November for DBG) for (a) NOR, (b) DBG, and (c) SCO.

sec to at least 5 Hz. The cause for the trend is probably associated with running water and local wave action that is suppressed in the winter months. The trend toward higher average power density in the winter months at periods between about 6 sec and at least 10 sec is also in agreement with the results of Lehmann (1952). This trend probably results from the unstable weather conditions in the winter months that give rise to numerous longer period microseism storms.

Station-to-Station Spectral Comparisons

Logarithmic averaged-power spectral-density curves at each station for the months of August and November are shown in Figure 3a and 3b, respectively. Both graphs show a low-noise-model spectra for reference (Peterson, 1989). During the month of August, the NOR and DBG spectra are similar, but the SCO spectra are systematically and significantly higher between about 6-sec periods and 3-Hz frequencies. All stations show spectral amplitudes similar to the low noise spectra from 10- to about 6-sec periods. From 6-sec periods to 5-Hz frequencies, all stations show spectral amplitudes well above the low-noise-model amplitudes. At about 5 Hz, the station spectral amplitudes are roughly a factor of 10 higher than the low-noise-model spectra.

The November spectra also show SCO to have systematically higher amplitudes between about 6-sec periods and 3-Hz frequencies. The NOR spectra, however, are systematically lower in amplitude between 10-sec periods and about 2-Hz frequencies than are the DBG spectra. Although the station spectra amplitudes are between a factor of 10 and 100 higher than the low-noise model between 10- and 3-sec periods, all station spectral amplitudes are within a factor of 5 of the low noise model between about 3- and at least 5-Hz frequencies.

Direction-of-Approach Comparisons

The direction of approach of microseism energy in the 8- to 4-sec period band was calculated every day at each station during the months of August and November, using a 5-min record beginning at 0300 GMT. We used a conventional closed-form P-wave backazimuth calculation method (Montalbetti and Kanasewich, 1970) and assumed Rayleigh wave polarization was dominant. A Hilbert transform was applied to the vertical component to convert the Rayleigh wave to an apparent P-wave polarization. We rejected only those days that had very poor polarization as determined by the magnitude of the backazimuth eigenvalue ratios (Jarpe and Dowla, 1991). These data were scaled by the value of the power in the 8- to 4-sec period band, determined by integrating the power density spectra for the 5-min vertical component record between 8- and 4-sec periods. The scaling was logarithmic using the following formula:

$$L = 50 + 100 \log \frac{P}{10^{-15}},$$

where L is the map scale length in kilometers, and P is the power in the 8- to 4-sec period band. Figure 4a and 4b shows the direction of approach during the months of August and November, respectively, with each vector length scaled by the above formula. The power difference between the shortest vectors and the longest vectors in the figures span more than three orders of magnitude.

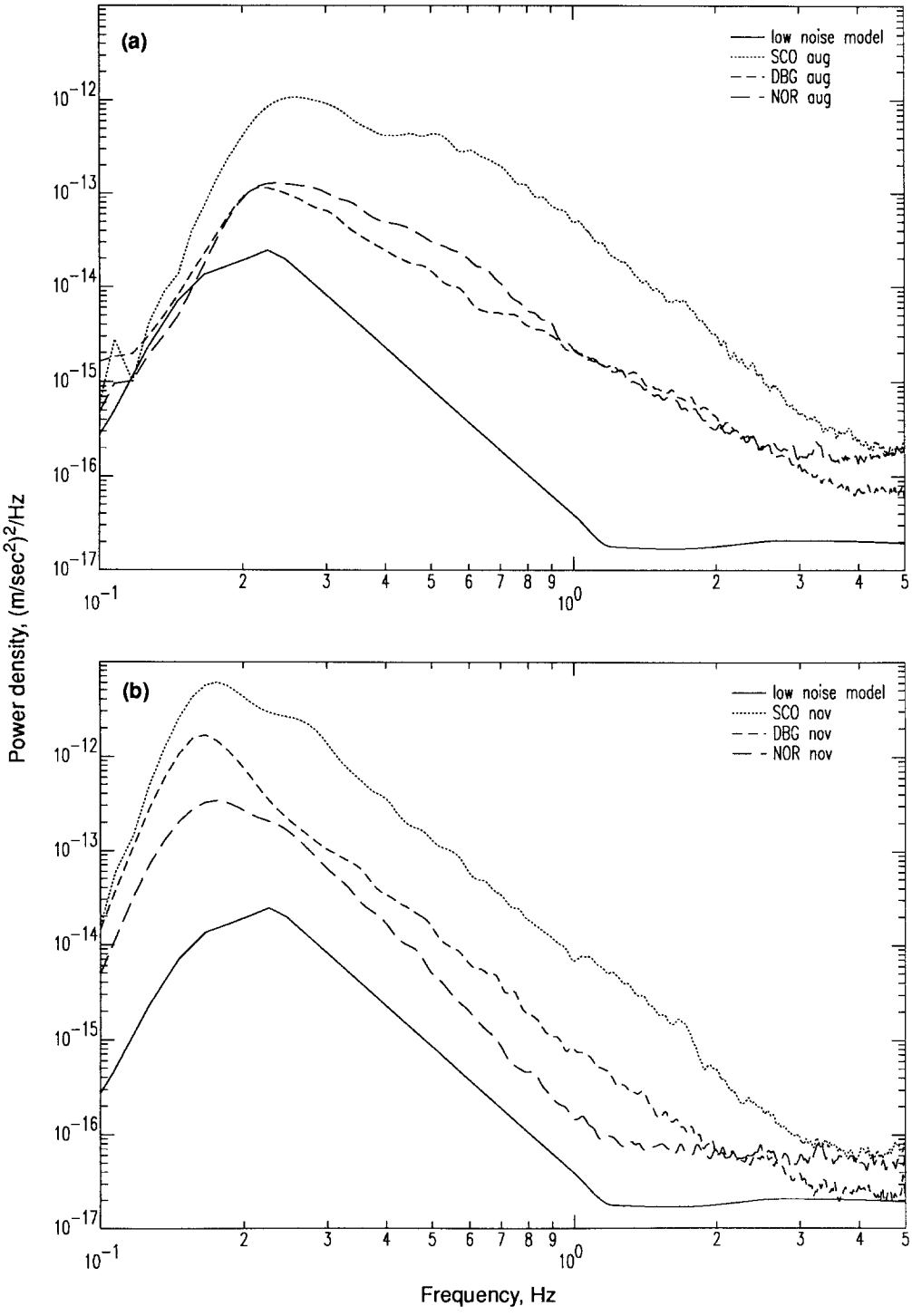

FIG. 3. The logarithmic averaged-acceleration power-density spectra station comparisons for (a) August and (b) November.

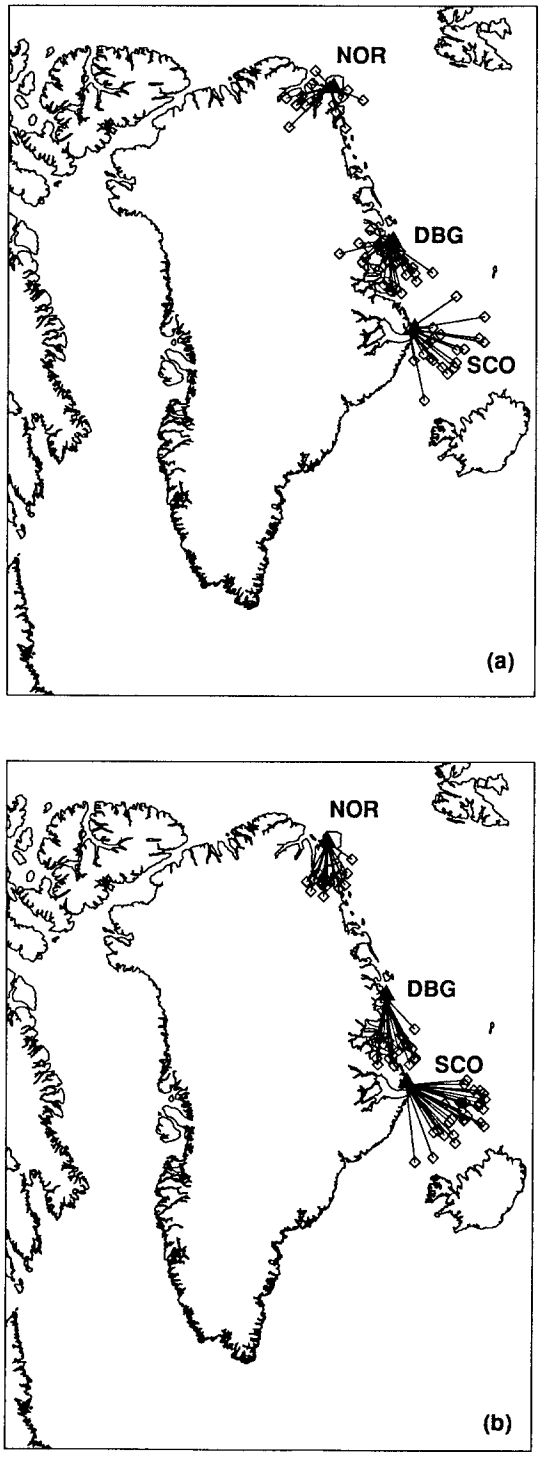

FIG. 4. Power-normalized direction of approaches at all three stations for the months of (a) August and (b) November.

The August results (Figure 4a) show significant scatter in the approach directions at NOR and DBG compared to SCO. It should be noted, however, that the microseism amplitudes are very low at NOR and are also low for many days at DBG. SCO has relatively high amplitude microseisms and less overall scatter. The mean approach directions for the three stations are 237° for NOR, 214° for DBG, and 142° for SCO.

The November results (Figure 4b) do not show any statistically significant difference in the approach means at the three stations but do show less scatter for NOR and DBG and higher amplitude microseisms at these stations as well. SCO shows similar scatter but higher average amplitude than in August. The mean approach directions for November are: 205° for NOR, 192° for DBG, and 142° for SCO.

The combined August and November direction-of-approach data for NOR and SCO are in reasonable agreement with the results of Jensen for these stations. NOR seems to be blind to microseisms originating in the Greenland Sea. NOR is dominated by microseisms with a source in the North Atlantic Ocean and a propagation path across almost the entire length of Greenland. DBG, although much closer to SCO than NOR, shows direction of approaches most similar to NOR. Although the average microseism amplitude at DBG is higher than at NOR, the direction of approach of microseisms at DBG strongly favors sources in the North Atlantic Ocean. Microseisms originating in the Greenland Sea (east to northeast of SCO) have similar propagation path lengths to DBG and SCO, but very few are recorded at DBG compared to SCO.

Direction of Approach During a Microseism Storm Period

During the period August 20 to 25, two microseism storms were recorded; one storm originated in Baffin Bay off the west Greenland coast and the other originated in the east Greenland Sea north of Iceland. The barometric pressure maps in Figure 5a to f show the weather conditions from August 20 to 25, respectively. The low barometric pressure and high pressure gradient off the west coast of Greenland shown on Figure 5a indicate the probability of high winds and significant microseism generation. This condition dissipates so that in Figure 5c a high pressure center is established over the west coast of Greenland. This condition is essentially maintained through Figure 5f with the exception of a minor low-pressure center shown in Figure 5d.

The weather pattern off the east coast of Greenland during August 20 to 25 is more complex. A relatively weak low-pressure center forms over Iceland (Fig. 5a) and moves northeast (Fig. 5b). A second low-pressure center forms between Iceland and the east Greenland coast (Fig. 5c). This center moves northeast and dissipates (Fig. 5d). Finally, a third low-pressure center forms off the east Greenland coast near the southern tip (Fig. 5e). This front remains stationary and intensifies with a relatively steep pressure gradient (Fig. 5f).

Spectral power in the 8- to 4-sec period band was computed on 5-min vertical component records taken every 3 hr at each station from August 20 to 25. The spectral powers are plotted in Figure 6. The spectral power and amplitude are very similar at all three stations between about the beginning of August 20 and the middle of August 21. After the middle of August 21 to about the beginning of August 23, SCO spectral power is much higher than NOR or DBG, the latter two showing similar spectral power during this time period. From the beginning of August 23 to nearly the end of August 24, NOR spectral power remains small

whereas both DBG and SCO show similar elevated spectral powers. By about the beginning of August 25, the three stations show roughly similar spectral power levels.

Direction-of-approach calculations in the 8- to 4-sec period band, using the methodology outlined earlier, were made using the same time periods that were

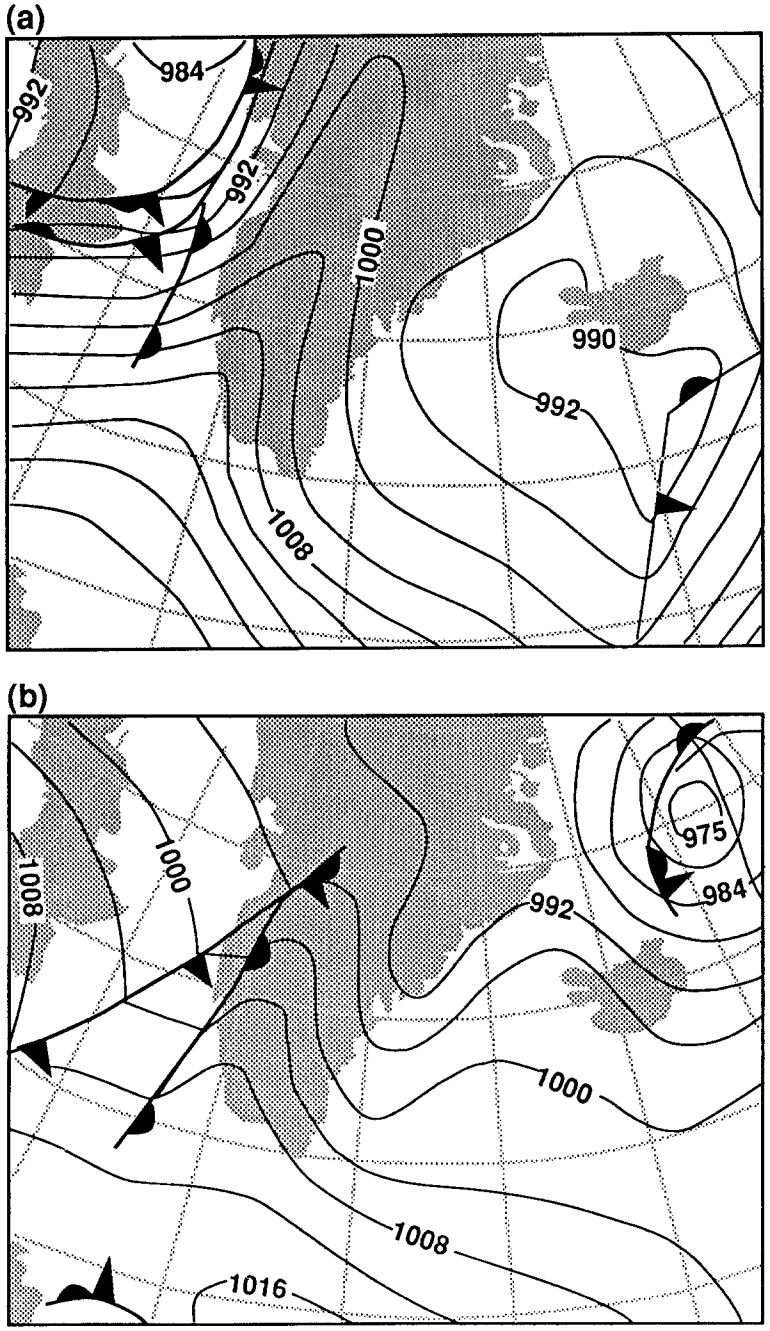

FIG. 5. Barometric pressure maps at 1200 GMT in the Greenland region are shown in (a) to (f) for the days August 20 to 25, respectively.

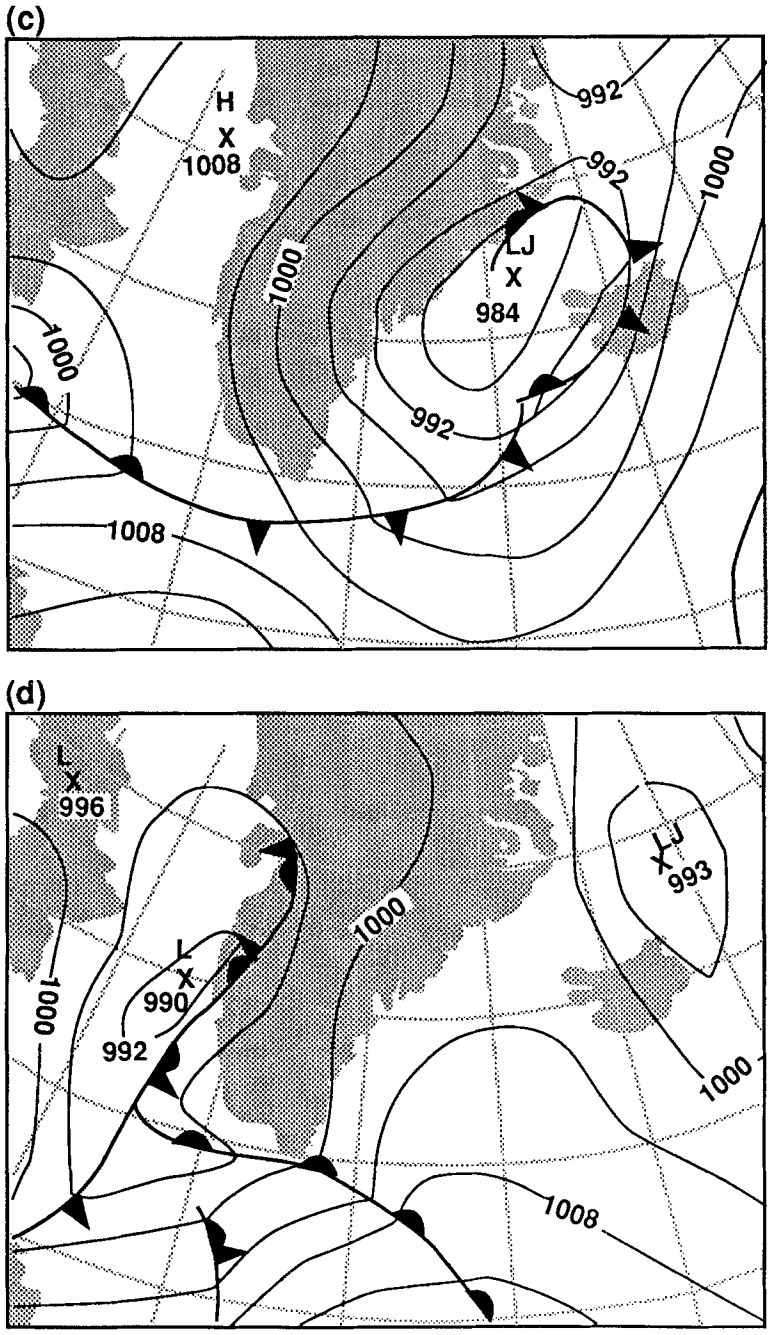

FIG. 5. (*Continued*)

used in the above spectral power determinations. The direction of approaches are plotted from two time periods: August 20 to mid-August 21 (Figure 7a) and August 23 to mid-August 24 (Figure 7b). These two time periods show very different direction of approaches at the three stations.

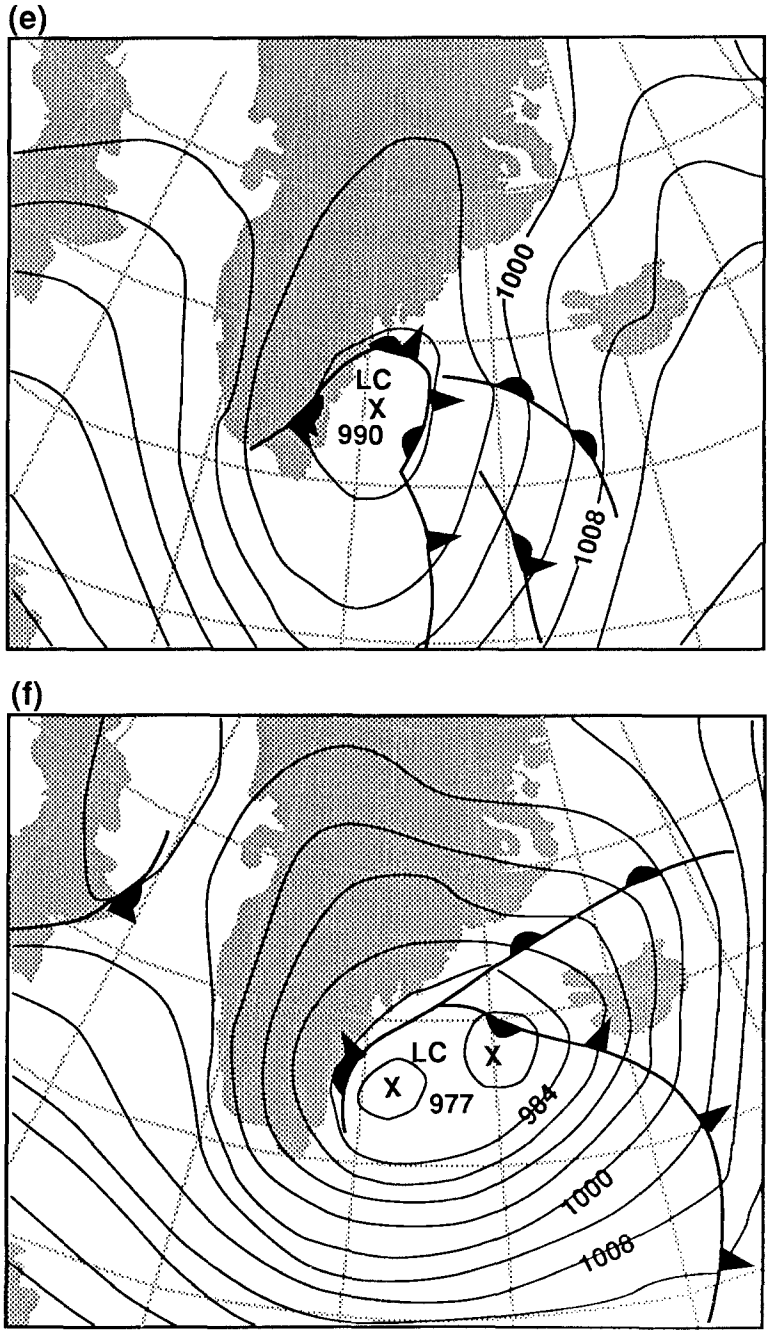

FIG. 5. (*Continued*)

The time period encompassed in Figure 7a corresponds to the time of a major low-pressure center with steep pressure gradients off the coast of west-central Greenland in Baffin Bay. The direction of approaches from NOR and DBG, with remarkable consistency, point in the direction of the west-central Greenland coast. SCO also points toward the west during some records but also points,

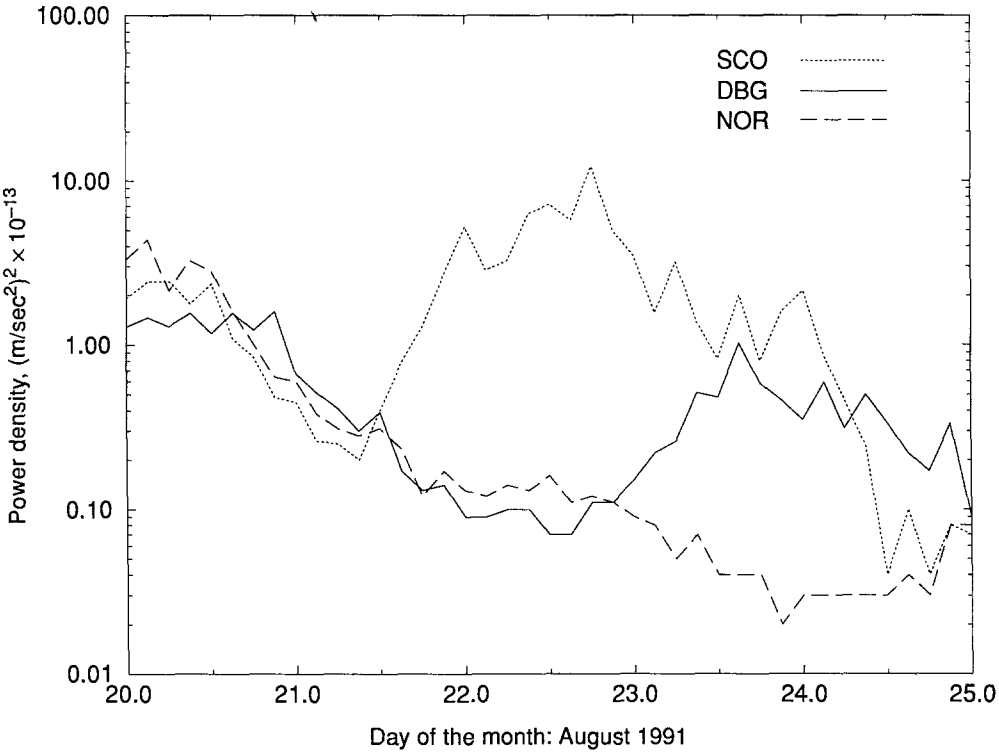

FIG. 6. Acceleration spectral power in the 8 to 4 sec period band, calculated for a 5-min time period every 3 hr from August 20 to 25, is shown for all three stations during the time period.

more typically, to the east during other records in the time period. It appears that SCO is receiving microseisms with roughly similar power from the east Greenland Sea and from Baffin Bay. Indeed, there is a mild low-pressure center in the Greenland Sea due east of SCO during this time period. Although DBG shows one record pointing to the east Greenland Sea, it appears to be dominated by the microseism source in Baffin Bay. NOR shows no apparent microseism energy from a Greenland Sea source.

Between August 23 and mid-August 24, low-pressure center forms and intensifies off the east Greenland coast between Greenland and Iceland with moderately steep pressure gradients. There is a very minor low-pressure center off the west coast of Greenland that dissipates. The direction of approaches from SCO and DBG consistently point to a source in the east Greenland Sea. Direction of approaches at NOR appear random. The very low spectral power levels during this time period and the poor polarizations obtained in the direction-of-approach calculations indicate that there is no measurable dominant microseism source received at station NOR during this time period.

The spectral powers and direction of approaches calculated during this storm period are consistent with the conclusions derived from daily noise power and direction-of-approach determinations. SCO is dominated by large microseisms originating in the east Greenland Sea. DBG records moderate microseisms from the east Greenland Sea but can be dominated by microseism sources originating in the south and west. NOR is blind to microseisms from the Greenland Sea. It only records microseisms from the south and south-west.

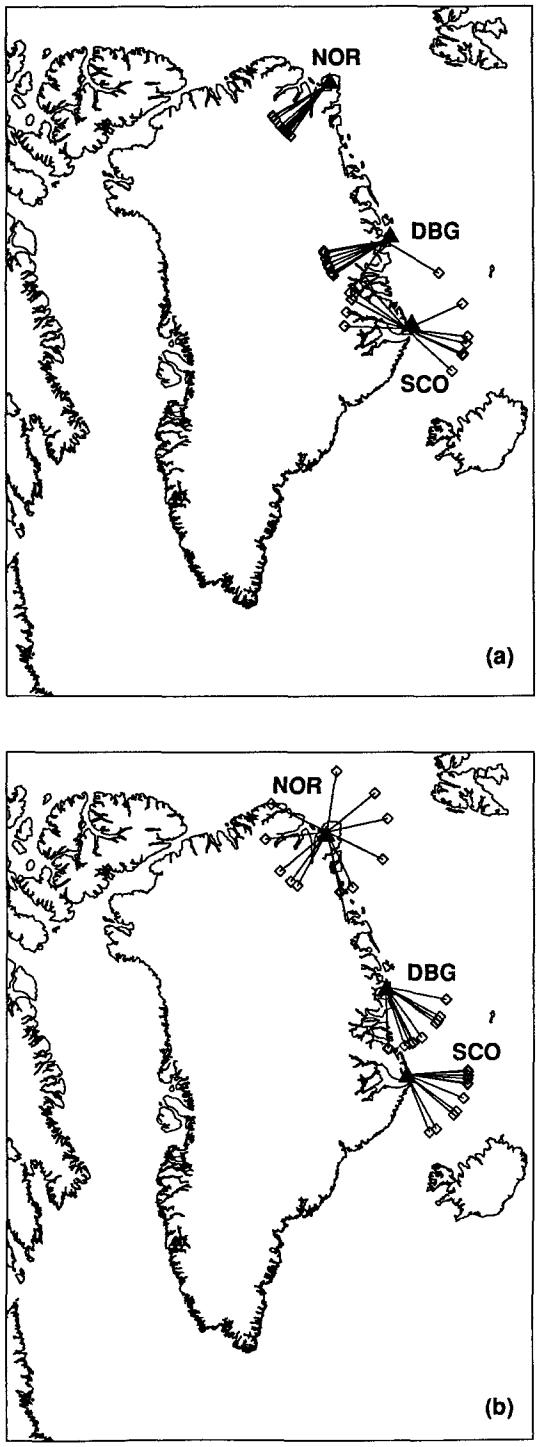

FIG. 7. Direction of approaches, calculated for a 5-min time period every 3 hr, is shown for all three stations for (a) August 20 at 0000 GMT through August 20 at 1200 GMT, and (b) August 23 at 0000 GMT through August 24 at 1200 GMT.

Oceanic Sediments and Microseism Propagation in Northeast Greenland

Oceanic sediments are the primary cause for the absence of short period (5 to 10 sec) surface waves in the seismograms recorded from mid-ocean ridge earthquakes in the Atlantic (Sykes and Oliver, 1964). The lack of short-period surface waves in the Atlantic is attributed to the greater thickness of sediments along the continental margins. Although short-period surface waves from mid-Pacific earthquakes are generally observed, their paths have an average sediment thickness of only a few tenths of a kilometer. So called "microseism barriers" may be caused by the presence of thick sediments along the propagation path.

Weidner (1975) studied four earthquakes that occurred on the mid-Atlantic ridge and concluded that sediments along the propagation path controlled surface-wave amplitudes and bandwidths. In particular, thick sediments (4 km and greater) can trap a significant fraction of short-period surface-wave (15 sec or less) energy and efficiently attenuate it. A quantity x/Q, where x is the propagation distance in kilometers, and Q is the shear wave quality factor, was defined as a measure of the attenuation expected at a given frequency and for a given sedimentary model. For typical thick sediment models, an x/Q of 10 shows attenuations as high as 20 dB at some frequencies. An x/Q of 100 can result in attenuations greater than 60 dB and over a larger bandwidth. Significant changes in sediment thickness along a propagation path (relative to a surface wavelength) can also result in reflection, scattering, and dispersion of the surface wave energy.

The northeast Greenland shelf extends north from about 72° N latitude, just north of Scoresbysund, to about 80° N latitude, just south of station NOR. This shelf varies in width from about 125 km in the south to about 300 km in the north. Sediment thicknesses on the shelf can only be inferred by aeromagnetic data and stratigraphic correlation because there are no seismic data available to date (Larsen, 1990). A sedimentary thickness map based on the available data (Jackson and Oakey, 1988) infers sedimentary deposits along the entire shelf, varying in thickness from 4 to 10 km. This corresponds to long-coast-parallel graben-ridge systems in the north and Tertiary volcanism in the south.

A seismic reflection profile, just south of the east Greenland shelf province, from Scoresbysund due east for about 125 km (Larsen and Jakobsdottir, 1988) shows sediment thicknesses between 1 and 3 km from the coast to about 80 km east. Between 80 and 125 km east of the coastline, the sediments thin to less than 1 km and continue to thin to around 0.2 km at about 175 km due east of the coast (Jackson and Oakey, 1988).

It seems likely that short-period surface-wave attenuation due to marine sediments in the east Greenland shelf is a major factor determining the observed direction of approaches. The track of typical storms giving rise to large microseisms in Scoresbysund form around Iceland and move northeast toward the northern coast of Norway. As noted earlier, such storms do not give rise to measurable microseisms in NOR and only occasional microseisms in DBG. For a typical storm track, the microseism propagation path to NOR through thick sediments will be large due to the physiography of the east Greenland shelf and the typical track of the microseism source. This path is probably between about 400 and 800 km. Assuming a Q of 15 (Weidner, 1975), this gives an x/Q of between 25 and 50. The paths to DBG are shorter (100 to 200 km), correspond-

ing to an x/Q of between about 7 and 15, but still significant. Although, strictly speaking, the Q values and sediment thicknesses on the east Greenland shelf are not known, values typical for the geological province and inferences based on other geophysical data and field geological correlations show that strong attenuation can be expected.

L_g waves from earthquakes in northeast Greenland between DAG and NOR recorded at SCO show abnormally high attenuation (Gregersen, 1982). These paths traverse a large section of the northeast Greenland shelf sedimentary basins, and those observations are therefore consistent with an oceanic sediment attenuation explanation for the observed microseisms in northeast Greenland.

Conclusions

The seasonal variation of seismic noise observed at stations NOR, DBG, and SCO are in agreement with earlier studies that were based on a more limited bandwidth. We observed the same trends at all three stations: a seismic noise minimum during the winter in the 3-sec period to 5-Hz frequency band and a seismic noise maximum during the winter in the 10- to 5-sec period band. The winter minimum at the relatively higher frequencies is probably due to the cessation of local wave and water action and local cultural activities. The winter maximum in the microseism frequency band is probably due to larger, more frequent storms at sea giving rise to larger, more frequent microseisms.

Direction of approaches of microseisms are in agreement with earlier studies at SCO and NOR. SCO records relatively large microseisms originating in the Greenland Sea and Denmark Strait, directly east to southeast. DBG records moderate amplitude microseisms originating primarily from the south, in the southern Denmark Strait and the North Atlantic Ocean. NOR records relatively small amplitude microseisms originating from the southern Denmark Strait, the North Atlantic Ocean, the Labrador Sea, and the Davis Strait. The relative blindness of DBG and the total blindness of NOR to microseisms originating in the Greenland Sea as recorded at SCO was shown for a specific storm period. During this period, NOR, DBG, and to a lesser extent SCO recorded microseisms associated with an atmospheric disturbance in the Davis Strait. Only SCO, and to a small extent DBG, recorded microseisms associated with a series of atmospheric disturbances in the Greenland Sea.

The east Greenland shelf, extending from about SCO to just south of NOR and extending from 125 km off the coast at the southern extremity to about 300 km north, is considered to contain sedimentary sequences varying from 4 to 10 km in thickness. Such thick sediments are known to strongly attenuate short-period surface waves. Because the range of microseism wave paths originating from most storms in the Greenland Sea traverse from 400 to 800 km of the northeast Greenland shelf sediments, strong wave attenuation can be expected. To a lesser extent, significant microseism attenuation should occur at DBG also. This is consistent with the observed microseism wave amplitudes and direction of approaches observed.

High-Arctic seismic stations seem to be unique locations from the perspective of broadband seismic noise. The lack of vegetation, running water (during most of the year), local wave action, and significant cultural activity result in a very low seismic noise environment at higher frequencies (about 1 Hz and above). Locations north of the perennial pack ice are protected from nearby microseism

generation because the presence of pack ice prevents the formation of standing waves at sea and coastal wave reflection. Furthermore, when stations are located near broad sedimentary basins, continental or ocean sea floor propagating microseisms from distant sources are strongly attenuated for paths traversing the basins. Such stations, although located on the coast (station NOR for example), can have seismic noise levels in the 10-sec to 1-Hz band as low as the lowest noise continental stations. Seismic stations located at some of these extreme latitudes could have very low average seismic background noise and very high average body-wave detectabilities over a broad seismic frequency band. This could be useful for a global nuclear test ban seismic monitoring network and for fundamental seismology studies.

ACKNOWLEDGMENTS

We are indebted to Don Rock for his support during field installation of the new seismic stations. We also which to thank the operators at stations Nord, Daneborg, and Scoresbysund for their ongoing efforts in maintaining the stations and distributing the data. We owe thanks to Jorgen Hjelme and Don Springer for their early support of this effort. We thank the Controller of Her Britannic Majestys Stationery Office for permission to reproduce the weather charts included in the manuscript. Finally, we are indebted to Elaine Price for editing of the manuscript and to Peter Goldstein for technical review. This work was performed under the auspices of the U.S. Department of Energy by Lawrence Livermore National Laboratory under Contract No. W-7405-Eng-48.

REFERENCES

Båth, M. (1953). Comparison of Microseisms in Greenland, Iceland, and Scandinavia, Meteorologiska Institionen Vid Kungl. Universitetet Uppsala Meddelande N:0 32, Reprinted from: *Tellus* **5**(2), 109–134.

Basham, P. W. and K. Whitham (1966). Microseism noise on Canadian seismograph records in 1962 and station capabilities, *Publ. Dominion Obs.* **32**(4), 123–135.

Gregersen, S. (1982). Seismicity and observations of L_g wave attenuation in Greenland, *Tectonophysics* **89**, 77–93.

Hasselmann, K. (1963). A statistical analysis of the generation of microseisms, *Rev. Physics* **1**(2), 177–210.

Hjortenberg, E. and J. Hjelme (1980). Seismic noise at Danish stations in relation to detection, *Publ. Inst. Geophys. Pol. Acad. Sc.* **A-9**(135), 103–107.

Hjortenberg, E. (1970). Direction of approach of *P* and Rayleigh Waves in the Greenland microseisms, *Extrait de la monographie 31 de l'Union Geodesique Internationale, Symposium Sur Les Microseisms*, pp. 27–31.

Jackson, H. R. and G. N. Oakey (1988). Sedimentary Thickness Map of the Arctic Ocean, *The Geology of North America*, Vol. L, Plate 5, The Arctic Ocean Region, Geological Society of America.

Jarpe, S. and F. Dowla (1991). Performance of high-frequency three-component stations for azimuth estimation from regional seismic phases, *Bull. Seism. Soc. Am.* **81**(3), 987–999.

Jensen, H. (1957). *On the Beat-Distribution in Group-Microseisms*, Danish Geodaetisk Institut, Meddelelse No. 34.

Jensen, H. (1958). *A Procedure for the Determination of Direction Of Approach of Microseism Waves*, Danish Geodaetisk Institut, Meddelelse No. 36.

Jensen, H. (1961). *Statistical Studies on the IGY Microseisms from Kobenhavn and Nord*, Danish Geodaetisk Institut, Meddelelse No. 39.

Jensen, H. (1965). *Direction of Approach of Microseisms in Scoresbysund, Ivigtut, and Godhavn*, Danish Geodatisk Institute, Meddelelse No. 40.

Larsen, H. C. and S. J. Jakobsdottir (1988). Distribution, crustal properties, and significance of seawards-dipping sub-basement reflectors off E. Greenland, *Early Tertiary Volcanism and the Opening of the NE Atlantic*, Geological Society of London Special Publ. 39, 95–114.

Larsen, H. C. (1990). The East Greenland shelf, *The Geology of North America, Vol. L, The Arctic Ocean Region*, Geol. Soc. Am. Bull., 185–210.

Lehmann, I. (1952). On the microseism movement recorded in Greenland and its relation to atmospheric disturbances, Extrait du volume *La Semaine d'etude sur le Probleme des Microseismes*, Pontificiae Academiae Scientiarvm Scripta Varia, Ex Aedibvs Academicis in Civitate Vaticana, 1–37.

Longuet-Higgins, M. S. (1950). A theory of the origin of microseisms, *Phil. Trans. Roy. Soc. London A*, 243, pp. 1–35.

MacDowall, J. (1959). A note on the relation between wind velocity and the amplitude of microseisms on the coast of antarctica, *Geophys. J. R. Astr. Soc.* **2**, 364–368.

Montalbetti, J. F. and E. R. Kanasewich (1970). Enhancement of teleseismic body waves with a polarization filter, *Geophys. J. R. Astr. Soc.* **21**, 413–416.

Peterson, J. (1989). *IRIS/USGS Plans for Upgrading the Global Seismograph Network, U.S. Geol. Surv. Open-File Rept. 89–471.*

Rodgers, P. W. (1991). *Frequency Limits for Electromagnetic and Feedback Seismometers as Determined from Signal-to-Noise Ratios*, Lawrence Livermore National Laboratory, Livermore, CA, UCRL-JC-107082.

Sykes, L. R. and J. Oliver (1964). The propagation of short-period seismic surface waves across oceanic areas Part II—Analysis of Seismograms, *Bull. Seism. Soc. Am.* **54**(5), Part A, 1375–1415.

Weidner, D. J. (1975). The effect of oceanic sediments on surface-wave propagation, *Bull. Seism. Soc. Am.* **65**(6), 1531–1552.

LAWRENCE LIVERMORE NATIONAL LABORATORY
LIVERMORE, CA 94550
(P.E.H.)

KORT-OG MATRIKELSTYRELSEN
(DK-2400, KOBENHAUN)
OFFICE OF SEISMOLOGY, DENMARK
(E.H.)

Manuscript received 2 November 1992